in Table I is approximately constant. An estimate of the fraction of dose absorbed as a function of time after opthalmic administration can be obtained from (10):

$$A_t/\text{Dose} = [C_t + k_1 AUC_{(0-t)} + (X_t)V_1^{-1}] \times V_1/\text{Dose} \quad \text{(Eq. 4)}$$

This equation was applied to the experimental data from t = 0–8 hr only, and the 24-hr points were determined separately from the dose-normalized AUC ratios. The fraction of dose absorbed as a function of time is presented in Fig. 3 for the 1 and 2% ophthalmic doses for the four animals using the parameters reported in Table II. From Fig. 3 it can be seen that absorption continues until at least 8 hr after administration for all animals at both doses. Furthermore, the fraction absorbed as a function of time does not appear to change for the two doses. The curves for animals 4 and 6 indicate a slower rate of absorption and appear to be flattening out at 8 hr, suggesting that absorption is essentially complete. The curves for animals 1 and 5 suggest that both the rate and extent of absorption is considerably greater.

The present study indicates that systemic absorption of I in the rabbit is slow and highly variable after ophthalmic administration. Prior work with rabbits demonstrates the possibility that both local and systemic mechanisms are involved in ocular pressure lowering (5, 6, 11). It would be desirable to have more detailed effect–time data together with plasma–time data in order to investigate possible I plasma–effect relationships. Clinical studies with glaucoma patients using both oral I and smoking marijuana cigarettes also show effective lowering of intraocular pressure. The pharmacodynamics is consistent with the clinical pharmacokinetics for both routes of administration, since the effect has a much slower onset and considerably longer duration for the oral study than occurs in the smoking study. The studies reported here do not differentiate local and systemic mechanisms. For ophthalmic administration, which should minimize systemic side effects, further work is needed to develop an effective dosage form (4).

REFERENCES

(1) J. C. Merritt, W. J. Crawford, P. C. Alexander, A. L. Anduze, and S. S. Belbart, *Ophthalmology*, **87**, 222 (1980).

(2) P. Cooler and J. M. Gregg, in "The Therapeutic Potential of Marijuana," S. Cohen and R. C. Stillman, Eds., Plenum, New York, N.Y., 1976. p. 77.

(3) J. C. Merritt, S. McKinnon, J. R. Armstrong, G. Hatem, and L. A. Reid, *Ann. Ophthalmol.*, **12**, 947 (1980).

(4) J. C. Merritt, D. D. Perry, D. N. Russell, and B. F. Jones, *J. Clin. Pharmacol.*, **21**, 467S (1981).

(5) K. Green, J. F. Bigger, K. King, and K. Bowman, *Exp. Eye Res.*, **24**, 197 (1977).

(6) K. Green and K. Bowman, in "The Pharmacology of Marijuana," M. C. Braude and S. Szara, Eds., Raven, New York, N.Y., 1976, p. 803.

(7) M. E. Wall, D. R. Brine, and M. Perez-Reyes, in "The Pharmacology of Marijuana," M. C. Braude and S. Szara, Eds. Raven, New York, N.Y., 1976, p. 93.

(8) M. E. Wall, D. R. Brine, J. T. Bursey, and D. Rosenthal, in "Cannabinoid Analysis in Physiological Fluids," J. A. Vinson, Ed., American Chemical Society, Washington, D.C., 1979, Chap. 3.

(9) J. D. Teale, J. M. Clough, E. M. Piall, L. J. King, and V. Marks, *Res. Commun. Chem. Pathol. Pharmacol.*, **11**, 339 (1975).

(10) M. Gibaldi and D. Perrier, "Pharmacokinetics," Marcel, New York, N.Y., 1975, Chap. 4.

(11) T. Krupin, C. Fritz, J. J. Dutton, and B. Becker, *Exp. Eye Res.*, **30**, 345 (1980).

ACKNOWLEDGMENTS

The experimental work was carried out at the Research Triangle Institute with funds from the National Institute on Drug Abuse under contracts HSM 42-71-95 to M. E. Wall and D. R. Brine, and N01-MH-1-0092 to K. H. Davis and J. Olsen.

Use of Metzler's NONLIN Program for Fitting Discontinuous Absorption Profiles

JAMES J. ZIMMERMAN

Received July 13, 1981, from the *Department of Pharmaceutics, School of Pharmacy, Temple University, Philadelphia, PA 19140.* Accepted for publication March 17, 1982. Present address: Clinical Research Department, Stuart Pharmaceuticals, Wilmington, DE 19897.

Abstract □ An alternative to the use of integral hybrid flow/compartmental model (HFCM) equations in fitting cases I and II discontinuous absorption profiles is presented. It is proposed that HFCM-integral equations be replaced by a system of differential equations in which sequential sets of equations describe the absorption profile from time zero to infinity. The required sets of differential equations for these two cases are presented as they apply to a two-compartment drug, potentially undergoing multiple absorption steps. It was shown that the use of the NONLIN program in the differential equation mode provides good fits for some unusually shaped absorption profiles of buformin, sulfisoxazole, and griseofulvin. The values of the parameter estimates and the sum of squared deviations, ΣSD, obtained with NONLIN were almost identical to those obtained with the FITSI2 program utilizing HFCM equations. While HFCM-integral equations required less computer time, they introduced the potential for negative absorption times. This problem is avoided by use of the differential equations method.

Keyphrases □ Absorption—fitting discontinuous profiles, use of NONLIN program □ NONLIN program—use for fitting discontinuous absorption profiles

Recently, discontinuous absorption processes in relation to linear pharmacokinetic models were reported (1). Integral equations for hybrid flow/compartmental models (HFCM) were derived for application to single- and multicompartment drugs exhibiting two special cases of discontinuous absorption.

In case I, absorption is assumed to begin at time t_1 and end at time t_2. The mathematical treatment of this case allows for a negative, zero, or positive value of t_1. Zero and positive values of t_1 have been used universally up to the present time in fitting data to equations for the extravascular administration of drugs exhibiting continuous absorption profiles (2). A positive t_1-value indicates the presence of an absorption lag time, while $t_1 = 0$ indicates the absence of a lag time. Negative values of t_1, however, have not been used previously and are difficult to rationalize. It was suggested that negative t_1 values obtained from computer fits using HFCM equations signify a rapid initial absorption phase (1). The absorption rate constant for this phase, however, is not estimable from these equations. Values of t_2 are always positive. When t_2 approximates the time to peak concentration, the absorption profile exhibits a discontinuity or sharp break, at which point the subsequent shape of the profile is governed only by the dispo-

0022-3549/83/0200-0138$01.00/0

Table I—Differential Equations Required in the DFUNC Subroutine of Metzler's NONLIN Program for Scheme I in Cases I and II Discontinuous Absorption Processes

Value of t_1[a]	Time Interval	Differential Equations	
		Case I: Absorption ceases at t_2	
<0	t_0–t_1'	$dX_a/dt = -k_{a1}X_a$	(Eq. 1)
		$dC_c/dt = k_{a1}X_a/V_c + k_{21}X_p/V_c - (k_{12} + k_{10})X_c/V_c$	(Eq. 2)
		$dC_p/dt = k_{12}X_c/V_c - k_{21}X_p/V_c$	(Eq. 3)
	t_1'–t_2	$dX_a/dt = -k_{a2}X_a$	(Eq. 4)
		$dC_c/dt = k_{a2}X_a/V_c + k_{21}X_p/V_c - (k_{12} + k_{10})X_c/V_c$	(Eq. 5)
		Eq. 3	
	t_2–t_∞	$dC_c/dt = k_{21}X_p/V_c - (k_{12} + k_{10})X_c/V_c$	(Eq. 6)
		Eq. 3	
0	t_1–t_2	Eqs. 1–3	
	t_2–t_∞	Eqs. 3 and 6	
>0	t_0–t_1	$dX_a/dt = 0$	(Eq. 7)
	t_1–t_2	Eqs. 1–3	
	t_1–t_∞	Eqs. 3 and 6	
		Case II: Absorption rate changes at t_2	
<0	t_0–t_1'	Eqs. 1–3	
	t_1–t_2	Eqs. 3–5	
	t_2–t_∞	$dX_a/dt = -k_{a3}X_a$	(Eq. 8)
		$dC_c/dt = k_{a3}X_a/V_c + k_{21}X_p/V_c - (k_{12} + k_{10})X_c/V_c$	(Eq. 9)
		Eq. 3	
0	t_1–t_2	Eqs. 1–3	
	t_2–t_∞	Eqs. 3–5	
>0	t_0–t_1	Eq. 7	
	t_1–t_2	Eqs. 1–3	
	t_2–t_∞	Eqs. 3–5	
		Combination of Cases I and II: Absorption rate changes at t_2 and ceases at t_3	
<0	t_0–t_1'	Eqs. 1–3	
	t_1–t_2	Eqs. 3–5	
	t_2–t_3	Eqs. 3, 8 and 9	
	t_3–t_∞	Eqs. 3 and 6	
0	t_1–t_2	Eqs. 1–3	
	t_2–t_3	Eqs. 3–5	
	t_3–t_∞	Eqs. 3 and 6	
>0	t_0–t_1	Eq. 7	
	t_1–t_2	Eqs. 1–3	
	t_2–t_3	Eqs. 3–5	
	t_3–t_∞	Eqs. 3 and 6	

[a] The parameter t_1 corresponds to the t_1-value permitted in the integral equations described previously (1).

sition of the drug. When t_2 is very large compared with absorption half-life, then the general equations reduce to those for the more typical case for continuous absorption (2).

In case II, t_1 may also assume a negative, zero, or positive value, but absorption does not end at t_2; it merely proceeds at a new rate. Consequently, two absorption rate constants are generated from the computer fit for the two sequential absorption phases. The absorption profile again shows a discontinuity at t_2, at which point there is a change in slope in the ascending region of the profile.

From a mechanistic point of view, case I discontinuities may represent situations where the absorption efficiency of the intestine reduces to zero at some location in the GI tract or where the release of drug from the dosage form abruptly ceases. Case II discontinuities may result from the existence of intestinal segments with different absorption efficiencies, or alternatively, from a change in the release characteristics of the formulation or from a pH-induced change in the concentration of absorbable drug species at the membrane site (1).

The usefulness of the HFCM equations was demonstrated (1) by obtaining nearly perfect fits for some unusual absorption profiles of griseofulvin (3), buformin (4), and sulfisoxazole (5). For each of these drugs, less exact fits were obtained when equations for continuous absorption were used in the fitting process.

The present report describes an alternative approach for the computer fitting of discontinuous absorption profiles. An alternative approach is needed that does not produce potentially negative absorption times as a result of the mathematical analysis. It is proposed that HFCM integral equations be replaced by a system of differential equations in which sequential sets of equations describe the absorption profile from time zero to infinity. It was shown that Metzler's NONLIN program (6), utilized in the differential equation mode, may be used to implement the proposed approach[1].

THEORETICAL

The use of Metzler's NONLIN program for implementing the proposed method for fitting discontinuous absorption profiles requires that a DFUNC subroutine be written employing differential equations[2]. Prior to writing the subroutine, however, it is necessary to choose an appropriate kinetic model, write differential equations for each species in the model, and correctly order the equations within the subroutine. The choice of kinetic model requires decisions with respect to both the compartmental and absorption characteristics of the drug. The compartmental characteristics may usually be obtained from previous studies or from a graphical treatment of the experimental data. Discontinuous absorption characteristics may be inferred from a graphical representation of the experimental data or from poor computer fits obtained using continuous absorption models. A correct ordering of the equations within

[1] The NONLIN program is available for use on (*a*) IBM (C. M. Metzler, The Upjohn Co., Kalamazoo, MI 40991) and (*b*) CDC (M. Rowland, Department of Pharmacy, University of Manchester, Manchester, M139PL, England) computers with the CDC version having the added advantage of providing residual plots and statistics for the residuals.

[2] While differential equations require more computer time than integral equations, the writing of DFUNC subroutines for discontinuous absorption processes is greatly simplified, particularly for complex models, when differential equations are used.

Table II—Parameter Values For The Fitting of Buformin Data [a]

Parameters	Values: HFCM Ref. 1 [b]	Values: HFCM FITSI2 [c]	Values: NONLIN [c]
k_{a1}, hr^{-1}	—	—	0.2509
k_{a2}, hr^{-1}	0.1836	0.1611	0.1580
k_{21}, hr^{-1}	0.05106	0.08804	0.07970
α, hr^{-1}	0.2362	0.2834	0.2719
β, hr^{-1}	0.0202	0.03441	0.03132
t_1, hr	−0.3016	−0.3119	—
t_1', hr [d]	—	—	0.50
t_2, hr	3.722	3.734	3.716
V_c/F, liters [e]	3203.4	79.582	79.343
D_0, μg [f]	100,000.0	100,000.0	100,000.0
ΣD^2	—	160.6	163.7
CP, sec [g]	—	2.58	4.93

[a] Data from Ref. 4. [b] Run on a PDP 11/10 computer. [c] Run on a CDC Cyber 174/2550 computer. [d] The parameter t_1' was a constant in NONLIN, and 0.50 hr is the time of the first blood sample after drug administration; $t_0 = 0$. [e] The parameter F is the systemic availability. [f] The parameter D_0 is the dose. [g] Fortran execution time without line printer plots and statistics for residuals.

the subroutine requires that the user follow instructions given in the NONLIN manual regarding the use of differential equations and that selected Fortran IF statements be employed to provide a logical kinetic flow while stressing the discontinuities. The development of a functional DFUNC subroutine is illustrated using Scheme I for a drug exhibiting known two-compartment characteristics and potential multiple absorption steps. The approach could be applied equally well to a drug characterized by either a fewer or a greater number of compartments.

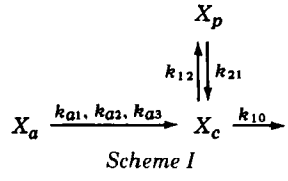

Scheme I

where X_a is the amount of drug at the absorption site; X_c is the amount of drug in the central compartment; X_p is the amount of drug in the peripheral compartment; k_{a1}, k_{a2}, and k_{a3} are the first-order absorption constants for the first, second, and third absorption steps, respectively; k_{12} and k_{21} are the first-order rate constants for the transfer of drug between compartments; and k_{10} is the first-order elimination constant.

Table I presents a summary of the systems of differential equations (Eqs. 1–9) associated with Scheme I for case I, case II, and combined cases I and II discontinuous absorption processes. For each of the cases, the differential equations are subgrouped further according to values of $t_1 < 0$, $= 0$, and > 0 and according to the time interval involved. The time-interval grouping introduces discontinuity into the model. Each time interval for a given initial value of t_1 corresponds to a different set of differential equations. For example, in case I ($t_1 < 0$), Eqs. 1–3 define absorption, distribution, and elimination (ADE) during the initial rapid absorption phase for the time interval, t_0–t_1', and Eqs. 3–5 describe the same events for the slower absorption phase from t_1' to t_2. Equations 3 and 6 describe the disposition of the drug after cessation of all absorption during the time interval, t_2–t_∞. The intervals, t_0–t_1' and t_1'–t_2, replace the single interval, t_1–t_2, reported previously (1). Since $t_0 = 0$, all absorption times are positive, and an absorption rate constant for the initial rapid absorption phase replaces a negative time constant. When data are scarce for the early absorption period, t_1' usually will be a constant taking on the time for the first blood sample after drug administration. For case I ($t_1 = 0$), the required set of differential equations includes Eqs. 1–3 for a single ADE cycle from t_1 to t_2 and Eqs. 3 and 6 for disposition for t_2 to t_∞. The required set of equations for case I ($t_1 > 0$) include those for case I ($t_1 = 0$) and Eq. 7, which accounts for the lag time from t_0 to t_1. For case II ($t_1 < 0$), Eqs. 1–3 and 3–5 represent the ADE processes for the first two absorption phases during the time intervals, t_0–t_1' and t_1'–t_2, respectively. These two intervals again replace the single interval, t_1–t_2. Equations 3, 8, and 9 represent the ADE processes for the third absorption phase from t_3 to t_∞. For case II ($t_1 = 0$) and case II ($t_1 > 0$), the required sets of differential equations involve an appropriate combination selected from Eqs. 1–5 and 7. Similarly, for the combination of cases I and II ($t_1 < 0$, $t_1 = 0$, $t_1 > 0$), the required sets of differential equations are chosen from Eqs. 1–9.

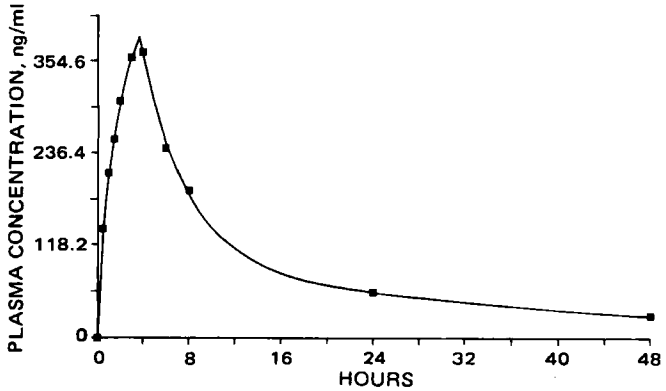

Figure 1—*Plasma concentration–time plot for the discontinuous fit of buformin data obtained with NONLIN. Key: theoretical (—); data points (■).*

Table III—Parameter Values For The Fitting of Sulfisoxazole Data [a]

Parameters	Values: HFCM Ref. 1 [b]	Values: HFCM FITSI2 [c]	Values: NONLIN [c]
k_{a1}, hr^{-1}	—	—	0.4082
k_{a2}, hr^{-1}	0.1080	0.1054	0.1063
k_{a3}, hr^{-1}	1.6788	1.5285	1.5363
k_{21}, hr^{-1}	0.1941	0.1833	0.1855
α, hr^{-1}	0.2938	0.2874	0.2879
β, hr^{-1}	0.08086	0.07853	0.07875
t_1, hr	−1.6656	−1.7104	—
t_1', hr [d]	—	—	0.50
t_2, hr	2.0807	2.000	2.000
V_c/F, liters [e]	10.749	10.604	10.907
D_0, mg [f]	2000.0	2000.0	2000.0
ΣD^2	—	0.83572	0.85284
CP, sec [g]	—	4.02	8.95

[a] Data from Ref. 5. [b] Run on a PDP 11/10 computer. [c] Run on a CDC Cyber 174/2550 computer. [d] The parameter t_1' was a constant in NONLIN, and 0.50 hr is the time of the first blood sample after drug administration; $t_0 = 0$. [e] The parameter F is the systemic availability. [f] The parameter D_0 is the dose. [g] Fortran execution time without line printer plots and statistics for residuals.

Equations 1–6 are written in a form consistent with the actual input quantities. Thus, Eqs. 2, 3, 5, and 6 are written in terms of concentrations. The latter conversions are made by dividing the rate expressions for X_c and X_p in Scheme I by V_c, the apparent volume of distribution for the central compartment. The concentration of drug in the peripheral compartment is also referred to the central compartment, since V_p, the apparent volume of distribution for the peripheral compartment, can only be estimated when experimental data for that compartment are available.

The ordering of differential equations within the DFUNC subroutine is accomplished by using the required NONLIN format (7) and selected IF statements for discontinuity[3].

EXPERIMENTAL

The version (*b*) of Metzler's NONLIN program[1] and a version of the FITSI2 program[4] for fitting discontinuous absorption data were obtained and made operational on a computer[5] by the university computer staff.

The data sets used in the computer fits were those used previously (1): griseofulvin (3), rat 11; buformin (4), patient 1; and sulfisoxazole (5) subject 3. Plots of the NONLIN computer fits were obtained with a plotter[6] and are reproduced as tracings in Figs. 1–3.

The initial estimates of the parameters used with both FITSI2 and

[3] The DFUNC subroutines used in fitting the data in Figs. 1–3 are available from the author upon request.

[4] R. Süverkrüp, Pharmazeutische Technologie, Pharmazeutisches Institut der Universität Bonn, Bonn, West Germany.

[5] CDC Cyber 174/2550.

[6] Calcomp.

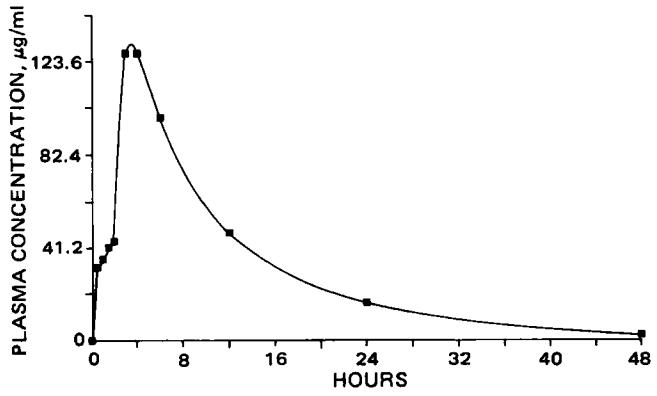

Figure 2—*Plasma concentration–time plot for the discontinuous fit of sulfisoxazole data obtained with NONLIN. Key: theoretical (—); data points (■).*

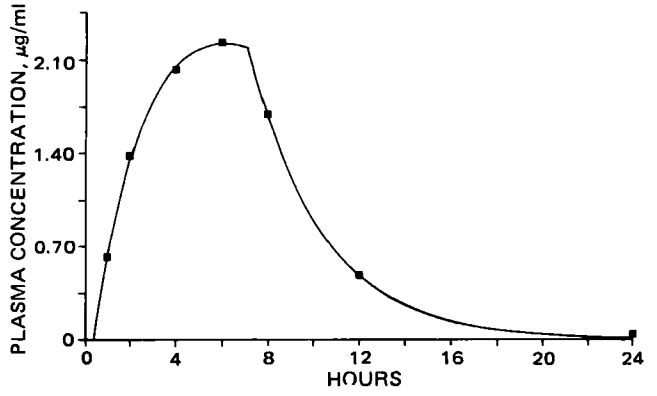

Figure 3—*Plasma concentration–time plot for the discontinuous fit of griseofulvin data obtained with NONLIN. Key: theoretical (—); data points (■).*

NONLIN were published values (1). The final estimates of the parameters were obtained by repeatedly entering the computed parameter values as initial estimates until the values stabilized.

In computer fits with NONLIN, the program default values for the parameters, DELINT, SSSTOP, and DELDER, were utilized. The DIG(I) parameter was set at 0.01, 0.001, and 0.001 to obtain the best fits for buformin, sulfisoxazole, and griseofulvin, respectively. All the data points shown in Figs. 1–3 were weighted equally.

RESULTS AND DISCUSSION

The results of the computer analyses of the three data sets are summarized in Tables II–IV and Figs. 1–3. In Tables II and III, parameter estimates obtained from NONLIN and FITSI2 are compared with those described previously (1). In both of these tables, values of α and β listed under NONLIN were calculated from quadratic relationships (8) using the NONLIN estimates of k_{12}, k_{21}, and k_{10}. In Table IV parameter estimates obtained from NONLIN are compared with those described previously (1). Less than perfect agreement between the two methods is expected since different algorithms are used in the two computer solutions and because Scheme I is not exactly the same model used previously (1).

Buformin (Case I: $t_1 < 0$)—The plasma data for buformin (4) in Fig. 1 was obtained in a diabetic patient after the oral administration of 100 mg of [^{14}C]buformin hydrochloride in a wax matrix. Based on first-order *in vitro* release characteristics of the dosage unit and two-compartment disposition characteristics *in vivo* (9), the data were fitted with NONLIN using a DFUNC subroutine for Scheme I, case I: $t_1 < 0$. The NONLIN estimates of k_{12} and k_{10} needed for calculating α and β were 0.116659 and 0.106853 hr^{-1}, respectively.

The model used in fitting the buformin data predicts two distinct absorption phases with absorption abruptly ending during the second and longer absorption time period. Accordingly, use of HFCM equations yields a negative value of t_1 and a positive value of t_2 as shown in columns 2 and 3 of Table II. An absorption rate constant, k_{a2}, is given for the second absorption phase but not for the short initial absorption phase. Use of the proposed differential equations method, however, provides absorption rate constants for both absorption phases and values for t_1' and t_2 as observed in column 4 of Table II. The estimated values of k_{12}, k_{21}, α, β, t_2, and V_c/F obtained with NONLIN (column 4) show closer agreement with values obtained with FITSI2 (column 3) run on a computer b^1 than with the published values (1) (column 2). However, the agreement in these parameters is not perfect for the described reasons. The extreme value of V_c/F in column 2 is apparently in error, since both NONLIN and FITSI2 gave much lower and almost identical estimates for this parameter.

Table IV—Parameter Values For The Fitting of Griseofulvin Data [a]

Parameters	Values HFCM[b] (Ref. 1)	Values NONLIN[c]
k_{a1}, hr^{-1}	0.09066	0.08944
k, hr^{-1} [d]	0.3090	0.3096
V_c/F, liters[e]	3.9393	3.9224
t_1, hr	0.3612	0.3308
t_2, hr	7.168	7.192
D_0, mg[f]	50.0	50.0
ΣD^2	—	0.001979
CP, sec[g]	—	2.43

[a] Data from Ref. 3. [b] Run on a PDP 11/10 computer. [c] Run on a CDC Cyber 174/2550 computer. [d] The parameter k is the elimination constant. [e] The parameter F is the systemic availability. [f] The parameter D_0 is the dose. [g] Fortran execution time without line printer plots and statistics for residuals.

Based upon the sum of squared deviations, ΣD^2, NONLIN and FITSI2 yielded almost identical fits to the data. It was observed, however, that NONLIN required more computer time for obtaining the parameter estimates than did FITSI2. The increased execution time with NONLIN is expected, since curve-fitting procedures using differential equations are inherently more time consuming than those using integral equations. The good fit provided by NONLIN is illustrated in Fig. 1.

Sulfisoxazole (Case II: $t_1 < 0$)—The plasma data for sulfisoxazole (5) in Fig. 2 was obtained from a healthy male subject after the oral administration of a 2.0-g tablet of sulfisoxazole. Because of the reported two-compartment behavior after intravenous administration (5), the data were fit with NONLIN using a DFUNC subroutine for Scheme I, case II: $t_1 < 0$. The NONLIN estimates of k_{12} and k_{10} required in calculating α and β were 0.0589257 and 0.122213 hr^{-1}, respectively.

The model used in fitting the sulfisoxazole data predicts three distinct absorption phases with absorption continuing sequentially throughout the three phases. The discontinuities in this case are incurred only by abrupt changes in the absorption rate, not by termination of absorption during the usual absorption period. Consequently, the use of HFCM equations yields a negative value for t_1 and a positive value for t_2, as listed in columns 2 and 3 of Table III. Columns 2 and 3 list estimates only of k_{a2} and k_{a3} for the second and third absorption phases. By contrast, the differential equations method (column 4) provides estimates of the absorption rate constants for all three absorption phases, together with values for t_1' and t_2.

The parameters in Table III estimated with NONLIN (column 4) show closer agreement with those obtained with FITSI2 (column 3) than those described previously (1) (column 2). For this data set, NONLIN yielded almost identical parameter estimates, but again, required more execution time for the discussed reasons. Based on the ΣD^2, almost identical fits were obtained with NONLIN and FITSI2. The exactness of the fit obtained with NONLIN is illustrated in Fig. 2.

The potential mechanisms for the irregular absorption profile for sulfisoxazole were discussed (5) (Fig. 2). Apparently, a small fraction of the 2.0-g dose dissolves rapidly to saturate the existing gastric fluid. A large fraction of the dose, however, remains as undissolved solid during its time in the stomach because of the small volume of fluid available for dissolution and the low membrane surface area available for absorption. Therefore, a rapid but limited absorption of this weak organic acid is possible from the stomach. Unabsorbed sulfisoxazole emptied into the small intestine undergoes a more rapid and complete absorption because of a more favorable pH for dissolution and an increased membrane surface area for absorption. Absorption phases 1 and 2 reflect gastric absorption, while absorption phase 3 reflects intestinal absorption.

Griseofulvin (Case I: $t_1 > 0$)—The plasma data for griseofulvin (3) in Fig. 3 was obtained in a rat after the oral intubation of 50 mg/kg of griseofulvin in a corn oil suspension. This data was fit with NONLIN using a modified DFUNC subroutine for Scheme I, case I: $t_1 > 0$, in which k_{12} and k_{21} equal zero.

The model used in fitting the data predicts a lag time before absorption begins and a single absorption phase that abruptly ends before absorption ceases. Accordingly, the use of HFCM equations yields positive values for both t_1 and t_2 and a value for the single absorption rate constant, k_{a1}, as observed in column 2 of Table IV. The proposed method in this case provides estimates of the same parameters, and there is good agreement between the estimates given in columns 2 and 3. The close-fitting plot obtained using NONLIN is given in Fig. 3.

REFERENCES

(1) R. Süverkrüp, *J. Pharm. Sci.*, **68**, 1395 (1979).

(2) M. Gibaldi and D. Perrier, "Pharmacokinetics," Dekker, New York, N.Y., 1975, Chaps. 1 and 2.

(3) P. J. Carrigan and T. R. Bates, *J. Pharm. Sci.*, **62**, 1477 (1973).

(4) V. H. Gutsche, L. Blumenbach, W. Losert, and H. Wiemann, *Arzneim.-Forsch.*, **26**, 1227 (1976).

(5) S. A. Kaplan, R. E. Weinfield, C. W. Abruzzo, and M. Lewis, *J. Pharm. Sci.*, **61**, 773 (1972).

(6) C. M. Metzler, G. L. Elfring, and A. J. McEwen, *Biometrics*, **30**, 562 (1974).

(7) C. M. Metzler, G. L. Elfring, and A. J. McEwen, "A Users Manual For NONLIN and Associated Programs," The Upjohn Co., Kalamazoo, Mich., 1976.

(8) M. Gibaldi and D. Perrier, "Pharmacokinetics," Dekker, New York, N.Y., 1975, Chap. 2.

(9) P. Botterman, A. Sovatzoglou, and U. Schweigart, in "Proceedings of the Second International Bigaunid Symposium," K. Oberdisse, H. Daweke, and G. Michael, Eds., Thieme, Stuttgart, West Germany, 1968.

ACKNOWLEGMENTS

The author acknowledges the assistance of the following members of the Temple University computer staff: Roslyn Gorin for procuring NONLIN; Liliane Clever for implementing NONLIN; Drusilla Gifford for implementing the Calcomp plots; and Bridget Peezick for implementing FITSI2.

The suggestion of Dr. C. M. Metzler for increasing the efficiency of the DFUNC subroutines used in this study is appreciated.

Kinetics and Thermodynamics of Interfacial Transfer

ROBERT FLEMING *, RICHARD H. GUY * § ×, and JONATHAN HADGRAFT ‡

Received January 13, 1981, from the **Department of Pharmaceutical Chemistry, The School of Pharmacy, University of London, London, WC1N 1AX, UK.* and the ‡*Department of Pharmacy, University of Nottingham, University Park, Nottingham, NG7 2RD, UK.* Accepted for publication March 25, 1982. §Present address: School of Pharmacy, University of California, San Francisco, CA 94143.

Abstract □ The kinetic barrier against the transport of methyl and ethyl nicotinates across the water–isopropyl myristate interface has been studied as a function of temperature using a rotating diffusion cell. The temperature dependence of the interfacial transfer kinetics has enabled calculation of the thermodynamic parameters for the process. It is evident from the results that, for the transferring solutes considered, the activation energy barrier is enthalpic, because there is a large positive entropy for transfer into the interfacial region.

Keyphrases □ Interfacial transfer—kinetics and thermodynamics, water–isopropyl myristate interface, methyl and ethyl nicotinates □ Kinetics—interfacial transfer thermodynamics, water–isopropyl myristate interface, methyl and ethyl nicotinates □ Thermodynamics—interfacial transfer kinetics, water–isopropyl myristate interface, methyl and ethyl nicotinates

An important physical process, common to all systems in which a solute transports from a high concentration aqueous phase across an organic membrane barrier into a low concentration aqueous phase, is the interfacial transfer of the substrate at the aqueous–organic and organic–aqueous interfaces. Few investigations into the kinetics and thermodynamics of interfacial transfer have been made, and the contribution of the phenomenon to overall membrane permeation has generally been assumed insignificant. However, recent studies have shown that transfer across the interfacial barrier can require a significant free energy input (1–3), and it is possible to identify circumstances for which the rate of interfacial transfer becomes the rate-determining step in membrane transport. For example, in the simplest case, consider the transport of drug molecules from an aqueous reservoir across an organic membrane into a perfect sink. Assuming that there is no stagnant diffusion layer in the aqueous reservoir phase, then the drug molecules must overcome two barriers so as to reach the sink on the far side of the membrane. These barriers are present due to interfacial transfer at the aqueous phase–membrane interface and due to diffusion through the organic membrane. The interfacial transfer is characterized by a heterogeneous rate constant k_{-1} (m/sec), which is related to the aqueous–organic partition coefficient of the drug (K) by the rate constant k_1 for interfacial transfer in the opposite direction (organic → aqueous), $K = k_1/k_{-1}$. Diffusion through the membrane is dependent upon the thickness of the membrane (l) and the diffusion coefficient of the drug in the membrane (D_{org}). Both processes also depend upon the cross-sectional area of the membrane. The relative contributions of the two components of the barrier may be compared by their reciprocal permeabilities [or resistivities (4)] and for interfacial transfer kinetics to have a significant effect on the overall rate of transport therefore requires:

$$1/Kk_{-1} \geq l/D_{org} \qquad \text{(Eq. 1)}$$

For certain small organic drug molecules, Kk_{-1} has been shown (1–3) to be $\sim 10^{-6}$ m/sec, and, taking a typical D_{org} of 10^{-10} m^2/sec, the inequality (Eq. 1) is satisfied by $l \leq 100$ μm. This degree of thickness is relevant not only to many biological membranes but also to emulsion systems and sustained-release formulations. Therefore, in neglecting slow interfacial transfer, it is possible that a major contribution to the transport rate-determining process in these systems is being ignored.

In this study, the kinetic barrier against interfacial transfer was investigated as a function of temperature. The

0022-3549/83/0200-0142$01.00/0